INTERNATIONAL JOURNAL FOR NUMERICAL AND ANALYTICAL METHODS IN GEOMECHANICS, VOL. 22, 133–149 (1998)

SHORT COMMUNICATION

THERMOELASTIC AND THERMOPLASTIC RESPONSE OF A DOUBLE-LAYER POROUS SPACE CONTAINING A DECAYING HEAT SOURCE

A. GIRAUD[1,*], F. HOMAND[1], G. ROUSSET[2]

[1] *Laboratoire de Géomécanique, E.N.S.G.-I.N.P.L., rue du Doyen Marcel Roubault, BP 40 54 501 Vandoeuvre-Les-Nancy, France*

[2] *Direction des Etudes et de La Recherche, DMTC, EDF Les Renardières, 77 250 Moret-sur-Loing, France*

SUMMARY

Solutions are presented for the behaviour of a layered porous space which contains a decaying heat source. Such a problem arises when high-level nuclear waste is placed in deep underground depositories in deep clayey formations of sedimentary basins. The geometry of the problem is one dimensional and the porous space is constituted by two layers: a deep low permeability layer which contains the nuclear waste disposal and a superficial layer. The solution is used to examine the effects of contrasts of permeability, thermal conductivity and specific heat capacities between the two layers on the large-scale behaviour of the porous space. Results are presented, using realistic data, for the pore pressure and temperature evolution at the heat source centre, and for the vertical displacement of the ground level. The superficial layer has no significant effects on pore pressure, temperature and stress evolution near the heat source centre. The vertical displacement of the ground level is mainly due to the thermal dilatation of the pore water, so it decreases with an increasing of permeability of the superficial layer. The solution of the time-dependent problem is carried out by applying Laplace transforms to the field variables, obtaining solutions and then using numerical methods to invert the transformed solutions. Comparisons with numerical simulations taking into account the non-linear and non-reversible behaviour of the rock mass are presented. © 1998 by John Wiley & Sons, Ltd.

Int. J. Numer. Anal. Meth. Geomech., Vol. 22, 133–149 (1998)
(No. of Figures: 8 No. of Tables: 2 No. of Refs: 32)

Key words: thermoporoelasticity; thermoporoplasticity; Laplace transform; Stehfest algorithm; finite element method

1. INTRODUCTION

The problem of deep storage of high-level radioactive waste in porous media such as clayey formations involves strong coupling effects between hydraulical, thermal and mechanical behaviour. An important security criterion taken into account for the choice of the material containing the heat storage is low permeability, in order to minimize the diffusion of radionucleids. Low-permeability porous materials such as deep clays are therefore studied in this problem.

*Correspondence to: A. Giraud, Laboratoire de Géomécanique, E.N.S.G. -I.N.P.L., rue du Doyen Marcel Roubault, BP 40 54 501 Vandoeuvre-Les-Nancy, France, E-mail giraudaensg.u-nancy.fr

CCC 0363–9601/98/020133–17$17.50

Giraud[1] shows that coupling effects between hydraulic and mechanical behaviour under the effect of a thermal loading are maxima in deep clays.

Recently, some authors have studied the large-scale behaviour of a porous rock mass containing a waste disposal site[2–4] comparing elastic and non-reversible rheological models. They show that the linear homogeneous isotropic thermoporoelastic behaviour is quite correct for the far-field analysis. The large-scale behaviour of the rock mass, e.g. the ground-level displacement, is little affected by complex thermomechanical behaviour of the deep material containing the heat storage (as thermal softening, see Reference 3) compared to the heterogeneity of thermal and mainly hydraulical properties. So this study is focused on the effect of a draining layer over the storage layer.

The first model used in this paper is fully linearized. The main hypothesis implies no convective heat transfer. The theory and the method of solution presented are most appropriate for relatively low permeable media (permeability approximately lower than $10^{-9}\,\mathrm{m\,s^{-1}}$).[5,1] The model takes into account the compressibility and the thermal expansion of both fluid and solid constituents.

The solutions for non-isothermal consolidation problems are difficult to obtain analytically, and may only be found for problems defined by simple geometries (one dimensional), simple boundary conditions, and linear thermoporoelastic model; see References 1, 2, 6–9. Semi-analytical methods have been developed by various authors to solve more complex and realistic problems under the hypothesis of linear behaviour. Those methods imply Fourier or Hankel transform to the field quantities along with a Laplace transform. The effect of the Fourier or Hankel transform is to reduce a two- or three-dimensional problem or one involving axial symmetry to one involving only a single spatial dimension.[10,11] Solutions are obtained in Fourier–Laplace or Hankel–Laplace transform space and numerically inverted.[11–13] Such methods are very useful for analysing multi-layer consolidation problems, for evaluating certain coupling effects in complex non isothermal consolidation problems, and for performing sensitivity analyses. Small and Booker[11] used this approach to present a solution for the problem of one-phase finite-layer thermoelastic soil containing a decaying heat source, and analysed the effect of thermal expansion coefficient heterogeneities between the layers. Savvidou and Booker[14] analysed the effect of anisotropic flow properties in a porous thermoporoelastic soil containing a heat source. More recently, Smith and Booker[15,16] presented methods of solving non-isothermal consolidation problems in linear thermoporoelastic materials based, respectively, on Green's functions and Boundary Element Method formulated in the Laplace transform domain.

The development of numerical methods based upon variational principles such as the Finite Element Method (FEM) have made it possible to analyse non-isothermal consolidation for much more complex conditions.[4,17–20]

This paper extends the previous analytical solution[2] of an homogeneous single thermoporoelastic isotropic layer containing a decaying heat source to a double layer. The solution method is then semi-analytical. Due to the geometrical hypothesis, the problem to solve is one dimensional and the spatial co-ordinate denotes the vertical level. It is therefore only necessary to apply Laplace transform (and not Fourier or Hankel transforms) to obtain a solution. A numerical inversion of the Laplace transform is performed.

2. GOVERNING EQUATIONS FOR THERMOPOROELASTICITY

The derivation of the equations governing the non-isothermal consolidation in linear isotropic porous thermoelastic medium was presented by the authors in a previous paper.[2] We assume

a quasi-static, infinitesimal deformation of macroscopically homogeneous and isotropic, fully saturated rocks with a connected pore structure. If solid and fluid phases are chemically inert and inertial forces are negligible, the complete set of differential equations for linear reversible behaviour (i.e. linear thermoporoelasticity; see References 16, 21, 22), can be written as

$$(K_0 + \tfrac{4}{3}G)\{\nabla\varepsilon_v\} - G\{\mathbf{rot}\}\{\mathbf{rot}\}\{\mathbf{u}\} - b\{\nabla P\} - 3\alpha_0 K_0\{\nabla\Theta\} = 0 \tag{1}$$

$$k\nabla^2 P = b\frac{\partial\varepsilon_v}{\partial t} + \frac{1}{M}\frac{\partial P}{\partial t} - 3\alpha_m\frac{\partial\Theta}{\partial t} \tag{2}$$

$$\lambda_T\Delta\Theta = 3\alpha_0 K_0 T_0\frac{\partial\varepsilon_v}{\partial t} - 3\alpha_m T_0\frac{\partial P}{\partial t} + C\frac{\partial\Theta}{\partial t} - Q_v \tag{3}$$

where $\{\mathbf{u}\}$ is the vector of displacement of matrix particles, $\varepsilon_v = \mathrm{Tr}([\varepsilon])$ denotes the volumetric strain, P is the excess pore pressure and Θ is the excess temperature. The linear isotropic thermoporoelastic model contains nine independent coefficients. G is the shear modulus, K_0 is the bulk modulus of drained solid, b is the Biot dimensionless coefficient of effective stress, M is the Biot bulk modulus of the fluid, k denotes the ratio between the permeability k_w ($m\,s^{-1}$) and the unit weight of the fluid $\gamma_w (k = k_w/\gamma_w)$, α_0 and α are, respectively, the drained and undrained expansion coefficients of matrix particles ($\alpha(K_0 + b^2 M) = \alpha_0 K_0 + \alpha_m bM$), λ_T is thermal conductivity of the porous medium, C is the volumetric specific heat, T_0 is a reference temperature and finally Q_v denotes the intensity of any distributed heat source ($W\,m^{-3}$).

Values of thermoporoelastic coefficients for clay and salt can be found in References 16, 23, 9, 3, 24. See also References 24–27 for a review of thermomechanical models for soft clays. In this paper, a set of values obtained for a low permeability European clay is presented (see Reference 2).

The equation of heat diffusion can be uncoupled for problems involving low gradients of fluid flow in low permeability media (permeabilities k_w lower than $10^{-9}\,m\,s^{-1}$; see Reference 1). The thermal diffusion equation (3) can be rewritten for convenience using the thermal diffusivity D_T:

$$\nabla^2\Theta = \frac{1}{D_T}\frac{\partial\Theta}{\partial t} = \frac{Q_v}{\lambda_T} \quad \text{where } D_T = \frac{\lambda_T}{C} \tag{4}$$

We will consider, for the superficial layer and the storage layer, permeabilities lower than 10^{-8}–$10^{-9}\,m\,s^{-1}$. Comparisons have been made with numerical results obtained with the finite element computer code THYME (see References 1 and 2) which take into account the coupling effects in equation (3). These coupling effects are negligible for all applications presented in this paper. An approximate discussion on the effect of convective heat transfer in a superficial high-permeability layer will be presented considering a simple particular case.

3. SOLUTION SCHEME FOR A DECAYING SOURCE IN A DOUBLE-LAYER ROCK MASS

3.1. Problem definition

Consider a heat source simulated by a layer of thickness $2a$ and depth d (d denotes the depth of the centre layer) in a semi-infinite double-layer porous rock mass (see Figure 1). The simulation represents the long-term thermohydromechanical behaviour of a nuclear waste repository site, on a large scale.

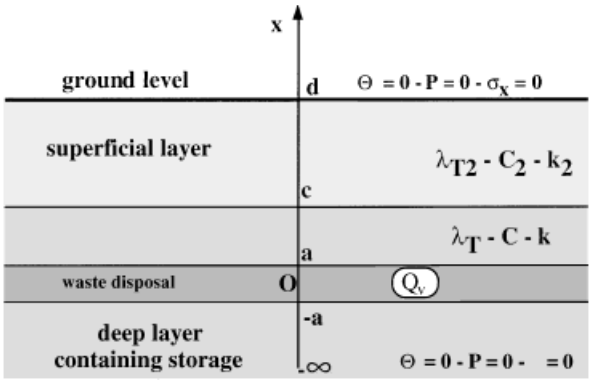

Figure 1. Geometry and boundary conditions

The problem is one-dimensional, characterized by the vertical spatial co-ordinate (denoted x). The vertical co-ordinate is at $x = 0$, at the heated layer centre, the interface between the deep layer containing the heat source and the superficial layer is at $x = c$ and the ground level at $x = d$. As a consequence of the geometrical hypothesis, the horizontal extension of the heated layer is infinite. The heat source is modelled by a volumetric heat production denoted Q_v ($W\,m^{-3}$), exponentially decreasing with time as is usually assumed for nuclear wastes:

$$Q_v(t) = Q_{v0}\,e^{-\omega t} \tag{5}$$

where ω is the decrease constant ($time^{-1}$) and Q_{v0} the initial thermal power.

Initial conditions:

$$u(x, t = 0) = 0, \qquad P(x, t = 0) = 0, \qquad \Theta(x, t = 0) = 0 \tag{6}$$

Boundary conditions: The porous rock-mass is semi-infinite, limited by the ground level, located at a finite distance from the heat source. Mechanical, hydraulic and thermal boundary conditions are imposed at ground level and at the infinite boundary as follows (see Reference 2 for more details):

Ground level ($x = d$):

$$\sigma_x(x = d, t) = 0, \qquad P(x = d, t) = 0, \qquad \Theta(x = d, t) = 0 \tag{7}$$

Infinite boundary ($x = -\infty$):

$$u(x = -\infty, t) = 0, \qquad P(x = -\infty, t) = 0, \qquad \Theta(x = -\infty, t) = 0 \tag{8}$$

Continuities of displacement, pore pressure, temperature, fluid mass flux and heat flux are imposed at the interface between the layers ($x = c$).

We take into account differences of thermal conductivity, specific heat and permeability (or hydraulic conductivity) between the two layers constituting the rock mass. Thermomechanical, hydromechanical and mechanical characteristics K_0, G, b, M, α_0, α are supposed identical for the two layers. λ_T, C and k denote, respectively, the thermal conductivity, the specific heat and the Darcy conductivity of the deep layer ($x \leqslant c$); λ_{T2}, C_2 and k_2 denote, respectively, the same quantities for the superficial layer ($c \leqslant x \leqslant d$). The problem is characterized by 17 independent parameters:

1. 12 constitutive parameters: K_0, G, b, M, α_0, α, λ_T, C, k, λ_{T2}, C_2 and k_2;
2. three geometrical parameters: the thickness of the heated layer ($2a$), the depth of the heat source centre (d) and the interface between the two layers (c);
3. two parameters for the thermal loading: Q_{v0} and ω.

The calculations presented in this paper concern the variations relative to an initial state. The linear thermoporoelastic theory enables these variations to be superposed on an initial arbitrary equilibrium state representing the initial mechanical, hydraulic and thermal conditions in rock-mass on a large scale.

The problem exhibits Cartesian symmetry and so the field quantities take the forms:

$$\{\mathbf{u}\}(x,t) = u(x,t)\{\mathbf{e}_x\}, \qquad P = P(x,t), \qquad \Theta = \Theta(x,t) \tag{9}$$

Dimensionless variables for time and space, t' and x', are introduced:

$$t' = \frac{t}{\tau_T}, \qquad x' = \frac{x}{a} \tag{10}$$

whereas

$$\tau_T = \frac{a^2}{4D_T}, \quad \omega' = \tau_T\omega, \quad u' = \frac{u}{a}, \quad d' = \frac{d}{a}, \quad c' = \frac{c}{a} \tag{11}$$

3.1. Thermal diffusion problem

The uncoupled thermal diffusion problem can be solved by introducing a non-dimensional temperature variation $\Theta'(x', t')$ and applying Laplace transform. Solutions of field equations (see Reference 2 for more details) can be written as

$$\begin{aligned}
c' \leqslant x' \leqslant d', \qquad & \bar{\Theta}'(x', s') = A(s')\mathrm{e}^{-r'x'} + B(s')\mathrm{e}^{r'x'} \\
1 \leqslant x' \leqslant c', \qquad & \bar{\Theta}'(x', s') = C(s')\mathrm{e}^{-q'x'} + D(s')\mathrm{e}^{q'x'} \\
-1 \leqslant x' \leqslant 1, \qquad & \bar{\Theta}'(x', s') = E(s')\mathrm{e}^{-q'x'} + F(s')\mathrm{e}^{q'x'} + \frac{1}{2s'(s'+\omega')} \\
\infty \leqslant x' \leqslant -1, \qquad & \bar{\Theta}'(x', s') = G(s')\mathrm{e}^{q'x'}
\end{aligned} \tag{12}$$

where

$$\Theta(x', t') = T_a\Theta'(x', t'), \qquad \bar{\Theta}'(x', s') = \int_0^\infty \mathrm{e}^{-s't'}\Theta'(x', t')\,\mathrm{d}t'$$

$$T_a = \frac{a^2}{2\lambda_T}Q_{v0}, \quad \beta_2 = \frac{D_T}{D_{T2}}, \quad q'^2 = 4s', \quad r'^2 = \beta_2 q'^2 \tag{13}$$

The seven unknown constants $A(s')$, $B(s')$, $C(s')$, $D(s')$, $E(s')$, $F(s')$, $G(s')$ can easily be determined considering the boundary condition $x' = d'$, and the six continuity conditions at $x' = c', \pm 1$. The solution is given in Appendix I. Among different algorithms useful to invert numerically Laplace transforms (see also Reference 29–31), we consider those developed by Stehfest[28] (with parameter $N = 18$). Comparison with the exact solution[2] shows that the Stehfest algorithm is relatively fast and give precise results.

3.2. Hydraulical diffusion problem and mechanical problem

A linear combination of the pore pressure variation P and the temperature variation Θ allows the mathematical hydraulical diffusion problem to simplified:

$$v = P + \varphi\Theta \tag{14}$$

where

$$\varphi = \frac{3\alpha_0 K_0}{b}\frac{\chi - 1}{\mu - 1}, \quad \chi = \frac{\alpha K}{\alpha_0 K_0}\frac{3K_0 + 4G}{3K + 4G}, \ \mu = \frac{D_H}{D_T}$$

$$D_H = k\frac{M(3K_0 + 4G)}{3K + 4G} \tag{15}$$

Introducing the non-dimensional variable $v'(x', t')$ and applying Laplace transform:

$$\bar{v}'(x', s') = \int_0^\infty e^{-s't'} v'(x', t')\, dt' \quad \text{where } v(x', t') = \varphi T_a v'(x', t') \tag{16}$$

the field equations of the hydraulical diffusion problem to solve can be written:

$$c' \leqslant x' \leqslant d', \quad \frac{\partial^2 \bar{v}'(x', s')}{\partial x'^2} - k'^2 \bar{v}'(x', s') - (\mu_2 - \mu) k'^2 \bar{\Theta}'(x', s') = 0 \tag{17}$$

$$1 \leqslant x' \leqslant c' \quad \text{and} \quad -\infty \leqslant x' \leqslant -1, \quad \frac{\partial^2 \bar{v}'(x', s')}{\partial x'^2} - h'^2 \bar{v}'(x', s') = 0 \tag{18}$$

$$-1 \leqslant x' \leqslant 1, \quad \frac{\partial^2 \bar{v}'(x', s')}{\partial x'^2} - h'^2 \bar{v}'(x', s') + \frac{2}{s' + \omega'} = 0 \tag{19}$$

Continuities of heat and fluid mass flux at the interface between the two layers give (the other continuity equations, more trivial, are not written)

$$\lim_{\varepsilon \to 0} \frac{\partial \bar{v}'}{\partial x'}(x' = c' - \varepsilon, s') = \lim_{\varepsilon \to 0} v_2 \left(\frac{\partial \bar{v}'}{\partial x'} - \left(1 - \frac{\delta_2}{v_2}\right) \frac{\partial \bar{\Theta}'}{\partial x'} \right)(x' = c' + \varepsilon, s') \tag{20}$$

where

$$\delta_2 = \frac{\lambda_{T2}}{\lambda_T}, \quad v_2 = \frac{k_2}{k}, \quad D_{H2} = v_2 D_H, \quad D_{T2} = \frac{\lambda_{T2}}{C_2}$$

$$\mu_2 = \frac{D_{H2}}{D_{T2}}, \quad h'^2 = \frac{4}{\mu} s', \quad k'^2 = \frac{h'^2}{v_2} \tag{21}$$

The solution of equations (17)–(19) is given in Appendix II.

Comment: the coupling terms appear in equations (17) and (20). Under the conditions $\mu_2 = \mu$ and $\delta_2 = v_2$, those coupling effects vanish so the hydraulical diffusion problem is mathematically identical to the thermal diffusion problem and the relations given by Giraud and Rousset[2] can be used, replacing function f_ω by Θ'.

Finally, the pore pressure variation P and the non-dimensional vertical displacement u' can be written (in Laplace transform):

$$\bar{P}(x', s') = \varphi T_a [\bar{v}'(x', s') - \bar{\Theta}'(x', s')] \tag{22}$$

$$\bar{u}'(x', s') = \frac{9\alpha_0 K_0}{3K_0 + 4G} T_a \left[\frac{\mu - \chi}{\mu - 1} \bar{I}'(x', s') + \frac{\chi - 1}{\mu - 1} \bar{J}'(x', s') \right] \tag{23}$$

where

$$\bar{I}'(x', s') = \int_{-\infty}^{X'} \bar{\Theta}'(u', s')\, du', \qquad \bar{J}'(x', s') = \int_{-\infty}^{X'} \bar{v}'(u', s')\, du' \tag{24}$$

4. NUMERICAL RESULTS AND DISCUSSION

We shall now present the results of a numerical example related to nuclear waste disposal technology and examine in particular the influence of a draining layer over the deep storage clayey layer. Consider a heat source with a thickness $2a = 10\,\text{m}$, at a centre depth $d = 230\,\text{m}$, a total initial heat output $Q_{v0} = 2\,\text{W m}^{-3}$ and a decrease constant $\omega = 0{\cdot}024\,\text{y}^{-1}$. This case was presented in Reference 2. Corresponding to the Mol experimental laboratory (230 ms below the ground level, in Boom clay, Belgium), we consider an interface between the deep layer and a highly permeable layer at $c = 50\,\text{m}$ (180 m depth, see Reference 3).

The thermal characteristic time constant τ_T, and the dimensionless constants ω', c' and d' are, respectively, $\tau_T \approx 121$ days, $\omega' = \tau_T \omega \approx 7{\cdot}97 \times 10^{-3}$, $c' = 10$ and $d' = 46$.

4.1. Analysis of pore pressure and displacement

The results are presented in Figure 2 showing the pore pressure distribution P and vertical displacement u at five different times: $t = 10$, 50, 100, 200 and 500 yr, for hydraulic permeability in the superficial layer varying from $k_{w2} = 4 \times 10^{-11}\,\text{m s}^{-1}$ to $k_{w2} = 10^3$, $k_w = 4 \times 10^{-9}\,\text{m s}^{-1}$. The corresponding temperature distribution is given in Figure 3 (left).

Table I. Parameters of the thermoporoelastic model for the two layers—reference case

Parameters	Deep layer	Superficial layer
Depth Z (m)	$180 \leqslant Z$	$0 \leqslant Z \leqslant 180$
Drained bulk modulus K_0 (MPa)	100	100
Shear modulus G (MPa)	60	60
Biot coefficient b	1·00	1·00
Biot bulk modulus M (MPa)	5500	5500
Permeability (m s^{-1})	$k_w = 4 \times 10^{-12}$	$k_{w2} = 4 \times 10^{-9}$
Specific heat ($\text{J m}^{-3}\,\text{K}^{-1}$)	$C = 2{\cdot}85 \times 10^6$	$C_2 = 2{\cdot}85 \times 10^6$
Drained coefficient of thermal dilatation α_0 (K^{-1})	$1{\cdot}0 \times 10^{-5}$	$1{\cdot}0 \times 10^{-5}$
Undrained coefficient of thermal dilatation α (K^{-1})	$4{\cdot}36 \times 10^{-5}$	$4{\cdot}36 \times 10^{-5}$
Thermal conductivity ($\text{W m}^{-1}\text{K}^{-1}$)	$\lambda_T = 1{\cdot}7$	$\lambda_{T2} = 1{\cdot}7$
Porosity	0·4	0·4
Skempton coefficient B	0·98	0·98
Undrained Poisson's ratio ν_u	0·495	0·495
Hydraulic diffusivity ($\text{m}^2\,\text{s}^{-1}$)	$D_H = 0{\cdot}697 \times 10^{-7}$	$D_{H2} = 0{\cdot}697 \times 10^{-4}$
Ratio of diffusivities	$\mu = 0{\cdot}12$	$\mu_2 = 0{\cdot}12 \times 10^3$
Coefficient χ	7·74	7·74

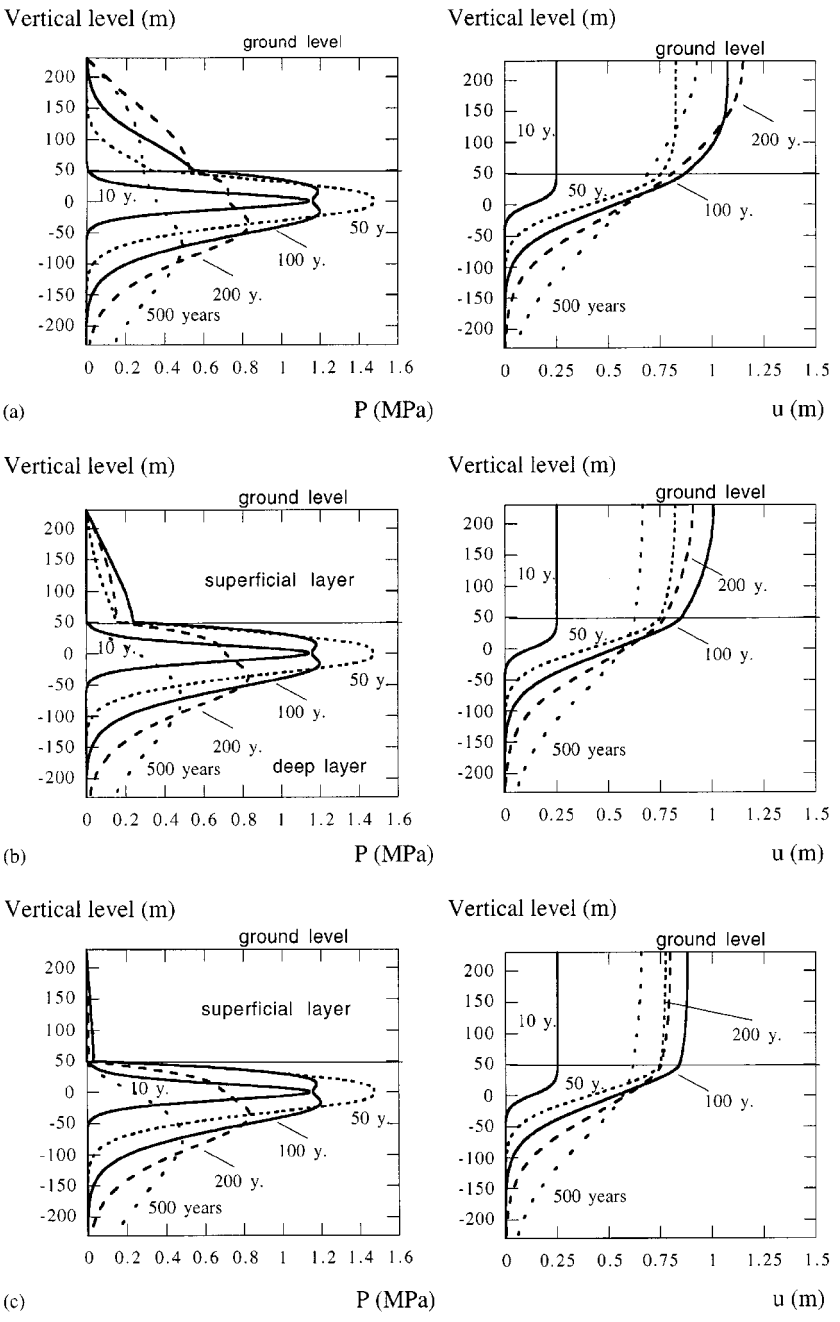

Figure 2. Pore pressure distribution and vertical displacement. (a) $k_{w2} = 10^{-11}\,\mathrm{m\,s^{-1}}$; (b) $k_{w2} = 10^{-10}\,\mathrm{m\,s^{-1}}$; (c) $k_{w2} = 10^{-9}\,\mathrm{m\,s^{-1}}$

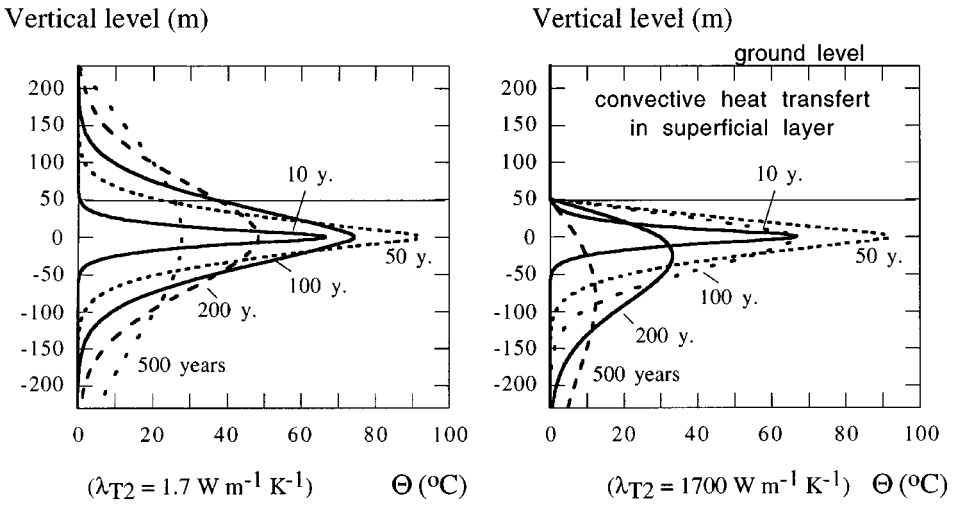

Figure 3. Temperature distribution

An increase in permeability in the superficial layer has no significant effect on pore pressure distribution near the centre of the heat source before approximately 100 yr. In particular, maximal pore pressure variation at the centre ($x = 0$) which occurs around 40 yr is not affected. At longer times, for $t = 200$ and 500 yr, an increase in permeability in the superficial layer accelerates the excess pore pressure decreasing in the deep layer, near the waste disposal.

The effect of an increase in permeability of k_{w2} on displacements of the superficial layer is not significant before 50 yr (100 yr for $k_{w2} = 10^{-11}\,\mathrm{m\,s^{-1}}$) and tends to diminish the displacements in the superficial layer at longer times.

4.2. *Analysis of vertical displacement of the ground level*

Consider the particular fictitious case of horizontal convective heat transfer in the superficial layer such that there are no temperature and pore pressure variations in the superficial layer, far from the interface ($x = c$). The model studied in this paper cannot take this case into account because displacements, water flow and heat flow are supposed to be vertical (geometrical hypothesis) and there are no non-linear convective coupling effects in heat diffusion equation (3). If we do not intend to model accurately thermal, hydraulic and mechanical evolutions near the interface $x = c$ but the mechanical behaviour of the ground level, a simple particular case can be useful (see Figure 4)

$$\frac{\lambda_{T2}}{\lambda_T} = \frac{k_{w2}}{k_w}$$

with $\lambda_{T2} = 1700\,\mathrm{W\,m\,K^{-1}}$, $k_{w2} = 4 \times 10^{-9}\,\mathrm{m\,s^{-1}}$, $\lambda_T = 1{\cdot}7\,\mathrm{W\,m\,K^{-1}}$, $k_w = 4 \times 10^{-12}\,\mathrm{m\,s^{-1}}$.

The thermal conductivity value of the superficial layer $\lambda_{T2} = 1700\,\mathrm{W\,m\,K^{-1}}$ is fictitious and not realistic. In this case, hydraulical diffusion problem is uncoupled and mathematically equivalent to the thermal diffusion problem. The analytical solution[2] of the homogeneous

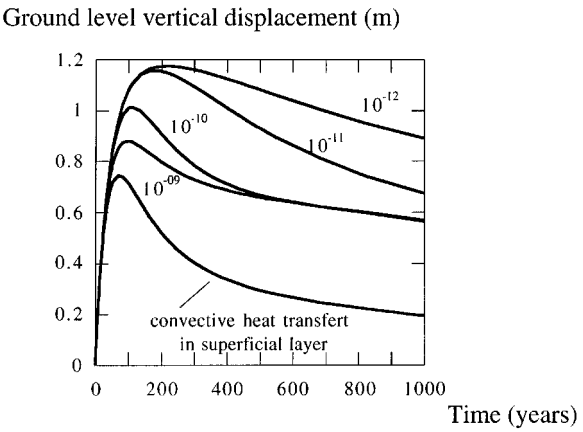

Figure 4. Evolution of ground level displacement. $k_{w2} = 10^{-12}$–$10^{-9}\,m\,s^{-1} - \lambda_{T2} = 1.7\,W\,m^{-1}K^{-1}$ and $k_{w2} = 10^{-9}\,m\,s^{-1} - \lambda_{T2} = 1700\,W\,m^{-1}K^{-1}$

Table II. Maximum vertical displacement of the ground level

	$u_{max}^{gr.l}(m)$	time (yr)
Analyt[2]; one layer λ_T; k_w; $d = 230\,m$	1·17	216
$\lambda_{T2} = \lambda_T$; $k_{w2} = 4 \times 10^{-11}\,ms^{-1}$	1·16	180
FEM; $\lambda_{T2} = \lambda_T$; $k_{w2} = 4 \times 10^{-11}\,m\,s^{-1}$	1·16	179
$\lambda_{T2} = \lambda_T$; $k_{w2} = 4 \times 10^{-10}\,m\,s^{-1}$	1·01	109
FEM; $\lambda_{T2} = \lambda_T$ $k_{w2} = 4 \times 10^{-10}\,m\,s^{-1}$	1·01	111
$\lambda_{T2} = \lambda_T$; $k_{w2} = 4 \times 10^{-9}\,m\,s^{-1}$	0·886	94.0
FEM; $\lambda_{T2} = \lambda_T$; $k_{w2} = 4 \times 10^{-9}\,m\,s^{-1}$	0·883	98.2
Analyt[2]; one layer λ_T; k_w; $d = 50\,m$	0·740	72.4
$\lambda_{T2}/\lambda_T = k_{w2}/k_w = 10^3$	0·746	72.2
FEM; $\lambda_{T2}/\lambda_T = k_{w2}/k_w = 10^3$	0·745	72.4

one-layer porous space containing a decaying heat source can also be used replacing $d = 230\,m$ by $d = c = 50\,m$.

We present in Table II comparison of maxima values of ground-level displacement (and time) for different characteristics obtained semi-analytically (or analytically in two cases) and numerically, using the finite element computer code THYME (see References 1 and 2). For calculations presented in this paper, we consider a mesh with 500 nodes (3000 degrees of freedom): 70 elements from $x = 230$ to 50 m (length varying from 8·86 m at $x = 230\,m$ to 0·31 m at $x = 50\,m$), 270 elements for $5\,m \leqslant |x| \leqslant 50\,m$ (length 0·33 m), 50 elements in the heat source $|x| \leqslant 5\,m$ (length 0·2 m) and 109 elements from $x = -50\,m$ to the infinity imposed at $x = -23,000\,m$ above the heat source to the ground level (length varying from 0·4 m at $x = -50\,m$ to 1700 m at $x = -23{,}000\,m$). For time integration, we use an implicit time stepping. We consider $\Delta t = \Delta t_0 = 2 \times 10^{-1}$ day for $t \leqslant 100$ days, and $\Delta t = 10^n \Delta t_0$ for 10^{1+n} days $\leqslant t \leqslant 10^{2+n}$ days (500 time steps between 10^{1+n} days and 10^{2+n} days).

Relative differences between maximal semi-analytical and finite element values of ground-level displacement are lower than 1 per cent. In the case $\lambda_{T2} = \lambda_T$, $k_{w2} = 4 \times 10^{-9}\,m\,s^{-1}$, the relative

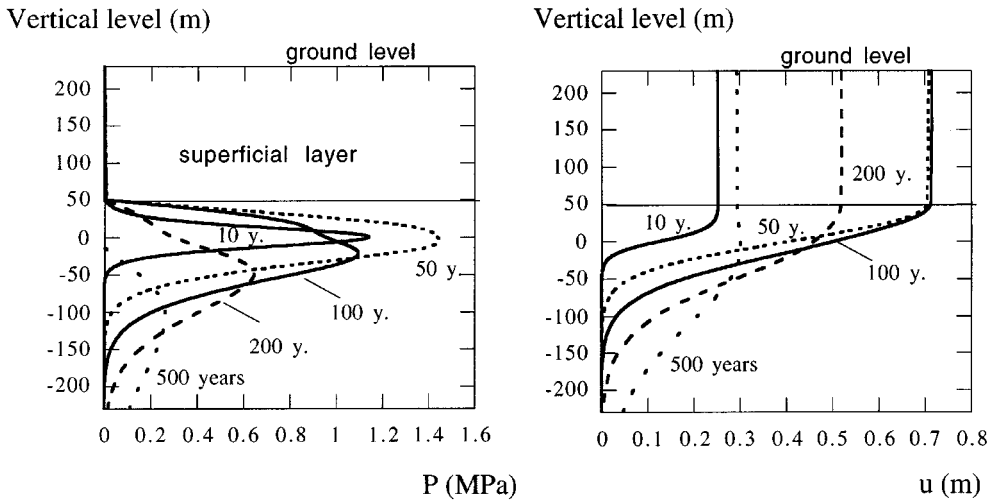

Figure 5. Pore pressure distribution and vertical displacement. $k_{w2} = 10^{-9}\,\mathrm{m\,s^{-1}} - \lambda_{T2} = 1700\,\mathrm{W\,m^{-1}\,K^{-1}}$

difference between time values reaches 4 per cent, whereas in other cases it is lower than 2 per cent (see Table II). The semi-analytical solution provides an interesting test for numerical finite element codes, especially for the transient evolution. Hypothesis of a single-layer low permeable porous space overestimates maximal displacement of the ground level and time to reach it. The influence of the permeability of the superficial layer on the ground-level displacement is significant. For example, an increase in permeability, from $k_w = k_{w2} = 4 \times 10^{-12}\,\mathrm{m\,s^{-1}}$ to $k_{w2} = 4 \times 10^{-9}\,\mathrm{m\,s^{-1}}$, tends to diminish the maximum value of ground-level displacement about 25 per cent. The effect is even more pronounced if there is convective heat transfer in the superficial layer (see Figure 5).

4.3. Effect of the non-reversible behaviour of the deep storage layer

On the basis of Picard's analysis[3] of the laboratory and *in situ* behaviour of Boom clay under thermal, hydraulical and mechanical loading, we consider a porous plastic model with thermal softening and Modified Cam Clay yield function (see Chapter IV of Reference[3] for a detailed description of the model). The yield function f takes the form:

$$f([\sigma^{ef}], p_c) = p'(p' + p_c) + \frac{q^2}{\mathbf{M}^2} \tag{25}$$

where $[\sigma^{ef}]$ and p_c denote respectively, the effective stress tensor and the apparent maximum past isotropic stress:

$$[\sigma^{ef}] = [\sigma] + P[\mathbf{1}]; \quad p' = \tfrac{1}{3}\,\mathrm{tr}[\sigma^{ef}]; \quad [\mathbf{s}] = [\sigma] - \tfrac{1}{3}\,\mathrm{tr}[\sigma][\mathbf{1}]; \quad q^2 = \tfrac{3}{2}[\mathbf{s}]:[\mathbf{s}] \tag{26}$$

At a depth of 220–250 m, near the Mol underground laboratory experiment, the preconsolidation pressure p_{c0} was estimated to be 5 MPa, corresponding to an initial mean effective stress of about $-2{\cdot}5$ MPa. This leads to very low effects of thermal hardening on a large scale. In order to

analyse the effects of plasticity and thermal hardening in optimal conditions, we consider an initial OverConsolidation Ratio (OCR) equal to 1: initial stress is supposed isotropic, and the initial mean effective stress p' is equal to the preconsolidation pressure p_{c0} (γ denotes the unit weight of the porous medium):

$$p_{c0}(x) = -(\gamma - \gamma_w)(x - 230) = -0{\cdot}01(x - 230)\,\mathrm{MPa\,m^{-1}} \tag{27}$$

Initial stress is located at the boundary of the elastic domain. According to Picard[3], the hardening law is defined by the relation

$$p_c = p_{c0}\exp[-v(\varepsilon_v^p + 3\alpha^p\Theta)], \quad v = 12{\cdot}6 \text{ and } \alpha_p = 10^{-4}\,\mathrm{K^{-1}} \tag{28}$$

and the strength parameter **M** value equals to 0·87. In order to compare elastic and plastic models more conveniently, elasticity was chosen linear for Modified Cam Clay model (see Table I for value of elastic parameters). Calculations without thermal softening ($\alpha^p = 0$) were also made to evaluate its effect. Calculations were performed using the finite element computer code THYME, the mesh and time steps are those previously defined.

The influence of plasticity on pore pressure evolution at the heat source centre is negligible: the only observed effect is a faster decreasing of excess pore pressure in the case of elastic behaviour with (fictitious) horizontal convective heat transfer in the superficial layer (see Figure 6). It is important to precise that large-scale modelling gives mean values of pore pressure evolutions. More realistic modelling of the near field around the heated storage should take into account another non-linear THM coupling effects in deep saturated clays, such as (for example) temperature and plasticity effects on permeability and thermal expansion (see References 3, 24, 25 and 26). The initial state before heating of the rock mass close to the underground storage structures such as galleries and wells (as in European concept) can be significantly disturbed by the excavation phase and the canisters emplacement and this should also be investigated in a near-field analysis.

Figures 7 and 8 present the distributions of plastic strain obtained, respectively, with and without thermal softening. The maximal plastic strain (vertical and volumetric) is located at the

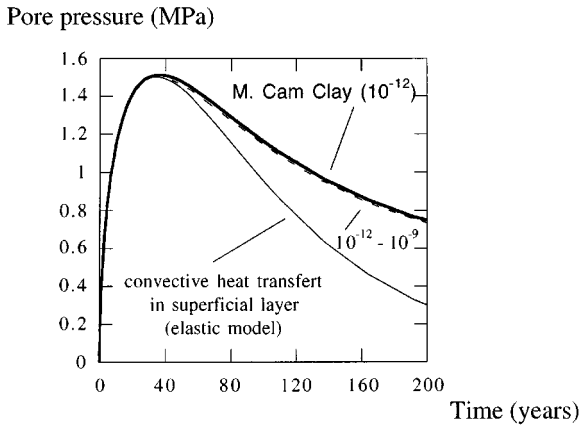

Figure 6. Pore pressure evolution at the centre of the waste disposal Thermoporoelasticity: $k_{w2} = 10^{-12} - 10^{-9}\,\mathrm{m\,s^{-1}} - \lambda_{T2} = 1.7\,\mathrm{W\,m^{-1}\,K^{-1}}$ and $k_{w2} = 10^{-9}\,\mathrm{m\,s^{-1}}$–$\lambda_{T2} = 1700\,\mathrm{W\,m^{-1}\,K^{-1}}$ Thermoporoelastoplasticity (Modified Cam Clay with thermal softening): $k_{w2} = 10^{-12}\,\mathrm{m\,s^{-1}} - \lambda_{T2} = 1.7\,\mathrm{W\,m^{-1}\,K^{-1}}$

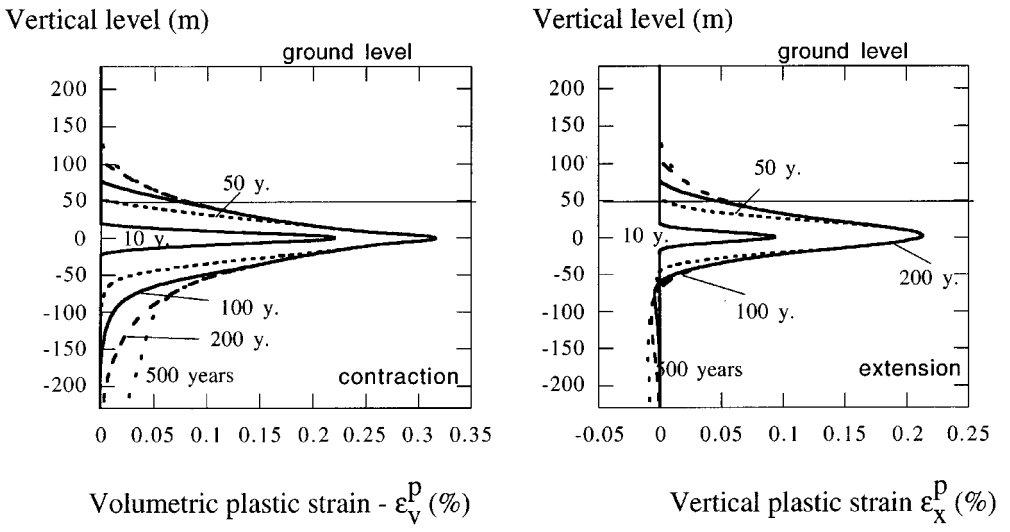

Figure 7. Volumetric and horizontal plastic strain distribution (model with thermal softening)

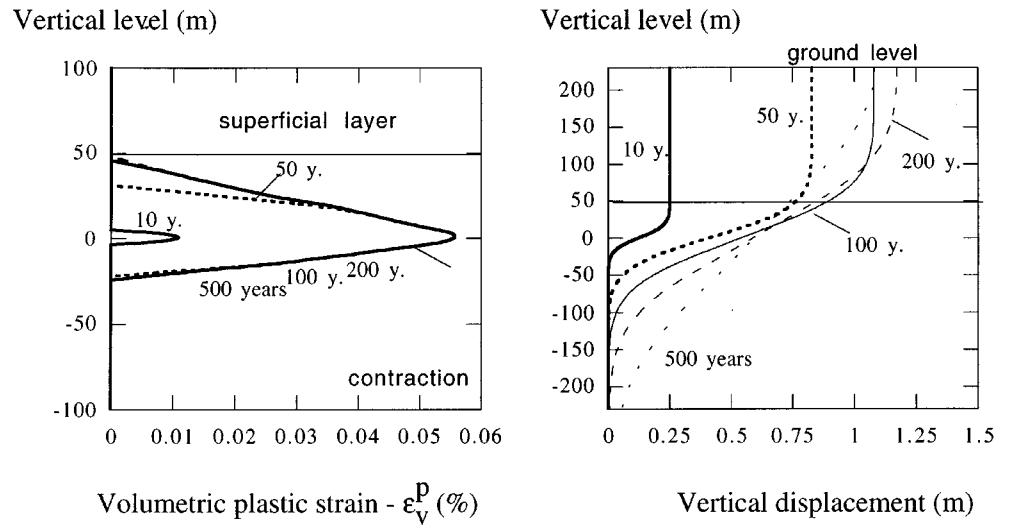

Figure 8. Volumetric plastic strain distribution and vertical displacement Thermoporoelastoplasticity: Modified Cam Clay without thermal softening

heat storage centre ($x = 0$) and the extension of the plastic zone is significant compared to the heat storage thickness, and strongly dependent on thermal softening. It can be noticed that the maximal extension of the plastic zone is obtained at the end of the increasing temperature phase (approximately 100 yr) for the plastic model without thermal softening, whereas the plastic model with thermal softening predicts an extension of the plastic zone (mainly below the heat storage) during the cooling phase.

Plasticity induces negative volumetric plastic strain ε_v^p (hardening) which has the opposite effect of thermal softening. This hardening tends to diminish the maximal extension of the plastic zone (compare Figures 7 and 8, left). Finally, it can be noticed that the effects of plasticity on the ground-level displacements are negligible, even with thermal softening and an initial OCR equal to 1. So a linear thermoporoelastic model is quite correct for the far-field analysis compare to the porous plastic models investigated (see also previous paper[2]).

5. CONCLUSIONS

The semi-analytical resolution method developed in this paper enabled the thermal and hydraulical heterogeneity effects on the large-scale (or far field) behaviour of a double-layer porous rock mass containing radioactive waste disposal site to be studied. The analysis focuses on the effects of contrast in permeability between the deep clayey layer containing the waste disposal and the superficial layer.

The mechanical behaviour of the ground level is mainly affected by the depth of the interface between the two layers, and not by the rheological behaviour of the rock mass near the waste disposal. Elastic models seem to be quite correct for modelizing large scale behaviour of the rock mass.

An extension of the analysis presented in this paper can be found using semi-analytical approaches involving Hankel or Fourier transforms on space variables: it will allow a more realistic geometry of the waste disposal site (for example 'thin cylinder' in axisymmetrical analysis), anisotropy of flow properties and thermal and mechanical properties, and a multi-layer porous space containing a deep waste disposal (see References 11 and 14) to be taken into account.

The Finite Element Method seems to be appropriate for analysing the effect of convective heat transfer in the superficial layer, and non-linear variation of permeability and water thermal expansion near the heat source.

APPENDIX I

Solution of thermal diffusion problem

$c' \leqslant x' \leqslant d'$:

$$\bar{\Theta}'(x',s') = \frac{1}{2s'(s'+\omega')} \frac{1}{1+\delta_2\beta_2^{1/2} - [1-\delta_2\beta_2^{1/2}]\exp[-2(d'-c')\beta_2^{1/2}q']}$$
$$\times (\exp[-(\beta_2^{1/2}x' - 1 + (1-\beta_2^{1/2})c')q'] - \exp[-(\beta_2^{1/2}x' + 1 + (1-\beta_2^{1/2})c')q']$$
$$- \exp[-(-\beta_2^{1/2}x' - 1 + (1-\beta_2^{1/2})c' + 2\beta_2^{1/2}d')q']$$
$$+ \exp[-(-\beta_2^{1/2}x' + 1 + (1-\beta_2^{1/2})c' + 2\beta_2^{1/2}d')q'])$$

$1 \leqslant x' \leqslant c'$:

$$\bar{\Theta}'(x',s') = \frac{1}{4s'(s'+\omega')}[\exp[-(x'-1)q'] - \exp[-(x'+1)q']]$$
$$+ \frac{\Omega(s')}{4s'(s'+\omega')}(\exp[-(-x'-1+2c')q'] - \exp[-(-x'+1+2c')q'])$$

$-1 \leqslant x' \leqslant 1$:

$$\bar{\Theta}'(x',s') = \frac{1}{4s'(s'+\omega')}(2 - \exp[-(x'+1)q'] - \exp[-(-x'+1)q'])$$
$$+ \frac{\Omega(s')}{4s'(s'+\omega')}(\exp[-(-x'-1+2c')q'] - \exp[-(-x'+1+2c')q'])$$

$-\infty \leqslant x' \leqslant -1$:

$$\bar{\Theta}'(x',s') = \frac{1}{4s'(s'+\omega')}(\exp[-(-x'-1)q'] - \exp[-(-x'+1)q'])$$
$$+ \frac{\Omega(s')}{4s'(s'+\omega')}(\exp[-(-x'-1+2c')q'] - \exp[-(-x'+1+2c')q'])$$

where

$$\Omega(s') = \frac{1 - \delta_2\beta_2^{1/2} - [1 + \delta_2\beta_2^{1/2}]\exp[-2(d'-c')\beta_2^{1/2}q']}{1 + \delta_2\beta_2^{1/2} - [1 - \delta_2\beta_2^{1/2}]\exp[-2(d'-c')\beta_2^{1/2}q']}$$

APPENDIX II

Solution of hydraulical diffusion problem

$$c' \leqslant x' \leqslant d': \quad \bar{v}'(x',s') = A_v(s')(\exp[-k'x'] - \exp[-(2d'-x')k'])$$
$$+ \frac{\mu_2 - \mu}{\beta_2\mu v_2 - 1}K(s')(\exp[-\beta_2^{1/2}x'q'] - \exp[-\beta_2^{1/2}(2d'-x')q'])$$

$$1 \leqslant x' \leqslant c': \quad \bar{v}'(x',s') = C_v(s')e^{-h'x'} + D_v(s')e^{h'x'}$$

$$-1 \leqslant x' \leqslant 1: \quad \bar{v}'(x',s') = E_v(s')e^{-h'x'} + F_v(s')e^{h'x'} + \frac{\mu}{2s'(s'+\omega')}$$

$$-\infty \leqslant x' \leqslant -1: \quad \bar{v}'(x',s') = G_v(s')e^{h'x'}$$

where

$$K(s') = \frac{1}{2s'(s'+\omega')}\frac{\exp[-(-1+(1-\beta_2^{1/2})c')q'] - \exp[-(1+(1-\beta_2^{1/2})c')q']}{1 + \delta_2\beta_2^{1/2} - [1 - \delta_2\beta_2^{1/2}]\exp[-2(d'-c')\beta_2^{1/2}q']}$$

The six continuity equations at $x' = c', \pm 1$ determine the six unknown constants A_v, C_v, D_v, E_v, F_v, G_v. The linear system to solve can be written in matrix form

$$\mathbf{MX} = \mathbf{F}, \quad \mathbf{M} \text{ is a } 6 \times 6 \text{ non-symmetric square matrix} \tag{29}$$

where (other matrix components equal to zero):

$$M_{11} = \exp[-k'c'] - \exp[-(2d'-c')k']; \; M_{12} = -\exp[-h'c']; \; M_{13} = -\exp[h'c']$$
$$M_{21} = -v_2k'(\exp[-k'c'] + \exp[-(2d'-c')k']);$$
$$M_{22} = h'\exp[-h'c']; \; M_{23} = -h'\exp[h'c']$$

$$M_{32} = M_{42} = M_{55} = M_{66} = -M_{34} = -M_{44} = -M_{56} = -M_{65} = \exp[-h']$$

$$M_{33} = M_{45} = M_{54} = M_{64} = -M_{35} = -M_{43} = \exp[h']$$

Unknown vector $\mathbf{X}$: $\mathbf{X}^{\mathrm{T}} = (X_1 = A_{\mathrm{v}}, X_2 = C_{\mathrm{v}}, X_3 = D_{\mathrm{v}}, X_4 = E_{\mathrm{v}}, X_5 = F_{\mathrm{v}}, X_6 = G_v)$

Right-hand side vector $\mathbf{F}$: $\mathbf{F}^{\mathrm{T}} = \left(F_1, F_2, F_3 = \dfrac{\mu}{2s'(s'+\omega')}, F_4 = 0, F_5 = -F_3, F_6 = 0\right)$

$$F_1 = -\frac{\mu_2 - \mu}{\beta_2 \mu v_2 - 1} K(\mathrm{s}')(\exp[-\beta_2^{1/2} c' q'] - \exp[-\beta_2^{1/2}(2d' - c')q'])$$

$$F_2 = v_2 \beta_2^{1/2}\left(\frac{\mu_2\text{-}\mu}{\beta_2 \mu v_2 - 1} - 1 + \frac{\delta_2}{v_2}\right) q' K(s')(\exp[-\beta_2^{1/2} c' q'] + \exp[-\beta_2^{1/2}(2d' - c')q'])$$

The linear system (29) is solved using a LU decomposition algorithm (see Reference 32, p. 38).

REFERENCES

1. A. Giraud, 'Couplages Thermo-Hydro-Mécaniques dans les Milieux Poreux Peu Perméables, Application aux Argiles Profondes, *Ph.D. Thesis*, ENPC, Paris, 1993.
2. A. Giraud and G. Rousset, 'Thermoelastic and thermoplastic response of a porous space submitted to a decaying heat source', *Int. J. Numer. Analyt. Meth. Geomech.*, **19,** 475–495 (1995).
3. J. M. Picard, 'Ecrouissage thermique des argiles saturées, Application au stockage de déchets radioactifs', *Ph.D. Thesis*, ENPC, Paris, 1994.
4. M. Ould, M. Amy and G. Rousset, 'Modélisation numérique en thermoporoélastoplasticité d'un stockage souterrain de déchets radioactifs en milieu argileux saturé. Application au calcul du champ lointain', *Revue Française Géotechnique* **69,** 1994.
5. M. Kurashige, 'A thermoelastic theory of fluid filled porous materials', *Int. J. Solids Struct.*, **25,** 1039–1052 (1989).
6. J. R. Booker and C. Savvidou, 'Consolidation around a spherical heat source', *Int. J. Solids Struct.*, **20,** 1079–1090 1984.
7. J. R. Booker and C. Savvidou, 'Consolidation around a point heat source' *Int. J. Numer. Analyt. Meth. Geomech.*, **9,** 173–184 (1985).
8. A. Giraud and G. Rousset, 'Consolidation around a volumic spherical decaying heat source', *J. Thermal Stresses*, **18,** 513–536 (1995).
9. D. F. McTigue, 'Thermoelastic response for fluid-saturated porous rock', *J. Geophys. Res.* **91,** 9533–9542 (1986).
10. J. R. Booker and J. C. Small, A method of computing the consolidation behaviour of layered soils using direct numerical inversion of Laplace transforms', *Int. J. Numer. Analyt. Meth. Geomech.*, **11,** 363–380 (1987).
11. J. C. Small and J. R. Booker, 'The behaviour of layered soil or rock containing a decaying heat source', *Int. J. Numer. Analyt. Meth. Geomech.*, **10,** 501–519 (1986).
12. T. Harnapattanapanich and I. Vardoulakis, Numerical Laplace–Fourier transform inversion technique for layered-soil consolidation problems—II: Gibson soil layer', *Int. J. Numer. Analyt. Meth. Geomech.*, **10,** 103–112 (1987).
13. I. Vardoulakis and T. Harnapattanapanich, 'Numerical Laplace–Fourier transform inversion technique for layered-soil consolidation problems—I: fundamental solutions and validation', *Int. J. Numer. Analyt. Meth. Geomech.*, **10,** 347–365 (1986).
14. C. Savvidou and J. R. Booker, 'Consolidation around a heat source buried deep in a porous thermoelastic medium with anisotropic flow properties', *Int. J. Numer. Analyt. Meth. Geomech.*, **13,** 75–90 (1990).
15. D. W. Smith and J. R. Booker, Green's functions for a fully coupled thermoporoelastic material', *Int. J. Numer. Analyt. Meth. Geomech.*, **17,** 139–163 (1993).
16. D. W. Smith and J. R. Booker, 'Boundary element analysis of linear thermoelastic consolidation', *Int. J. Numer. Analyt. Meth. Geomech.*, **20,** 457–488 (1996).
17. H. N. Seneviratne, J. P. Carter and J. R. Booker, 'Analysis of fully coupled thermomechanical behaviour around a rigid cylindrical heat source buried in clay', *Int. J. Numer. Analyt. Meth. Geomech.*, **18,** 177–203 (1994).
18. P. Dangla, 'Variational formulation of a thermoporomechanical problem', in P. Charlez (ed.), *Mechanics of Porous Media*, Balkema, Rotterdam, ISBN 90 5410 628 X, 1995.
19. J. F. Shao, 'Numerical solutions of non-linear problems related to thermal convection and poroplasticity', in P. Charlez (ed.), '*Mechanics of Porous Media*', Balkema, Rotterdam, ISBN 90 5410 628 X, 1995.

20. T. S. Nguyen and A. P. S. Selvadurai, 'Coupled thermal-mechanical-hydrological behaviour of sparsely fractured rock: implication for nuclear fuel waste disposal', *Int. J. Rock. Mech. Min. Sci. Geomech. Abstr.*, **32,** 465–479 (1995).
21. J. R. Rice and M. P. Cleary, Some basic stress diffusion solutions for fluid saturated elastic porous media with compressible constituents, *Rev. Geophys. Space Phys.* **14,** 227–241 (1976).
22. O. Coussy, *Mechanics of Porous Continua*, Wiley, New York, 1995.
23. C. Savvidou, Effects of a heat source in saturated clay, *Ph.D. Thesis*, Cambridge University, 1984.
24. H. N. Seneviratne, J. P. Carter, D. W. Airey and J. R. Booker, 'A review of models for predicting thermomechanical behaviour of soft clays', *Int. J. Numer. Analyt. Meth. Geomech.*, **17,** 715–733 (1993).
25. T. Hueckel and G. Baldi, 'Thermoplasticity of saturated clays: experimental study', *J. Geotech. Engng.*, **116,** 1778–1796 (1990).
26. T. Hueckel and M. Borsetto, 'Thermoplasticity of saturated clays and shales: constitutive equations', *J. Geotech. Engng.*, **116,** 1765–1777 (1990).
27. T. Hueckel and R. Pellegrini, 'Thermoplasticity modeling of undrained failure of saturated clay due to heating', *Soils Found.*, **31,** 1–16 (1991).
28. H. Stehfest, 'Numerical inversion of Laplace transforms', *Commun. Assoc. Comput. Mach.*, **13,** 47–49 (1970).
29. K. S. Crump, 'Numerical inversion of Laplace transforms using a Fourier series approximation', *J. Assoc. Comput. Mach.*, **23**, 89–96 (1976).
30. A. Talbot, 'The accurate numerical inversion of Laplace transforms', *J. Inst. Maths Appl.*, **23,** 97–120 (1979).
31. B. Davies and B. Martin, 'Numerical inversion of the Laplace transform, a survey and comparison of methods', *J. Comput. Phys.*, **33,** 1–32 (1979).
32. W. H. Press, S. A. Teukolski, W. T. Vetterling and B. P. Flannery, *Numerical Recipes in Fortran*, Cambridge University Press, Cambridge, 1992.

